

# Optical System Design for a Head-up Display Using Aberration Analysis of an Off-axis Two-mirror System

Byung-Hyun Kim and Sung-Chan Park\*

*Department of Physics, Dankook University, Cheonan 31116, Korea*

(Received June 30, 2016 : accepted July 25, 2016)

This study presents a new optical system for a combiner-type head-up display (HUD) with a cylindrical lens as an asymmetrical aberration corrector, instead of a freeform mirror. In the initial design process based on off-axial aberration analysis, we obtain an off-axis two-mirror system corrected for linear astigmatism and spherical aberration by adding a conic secondary mirror to an off-axis paraboloidal mirror. Thus, since the starting optical system for an HUD is corrected for dominant aberrations, it enables us to balance the residual asymmetrical aberrations with a simple optical surface such as a cylinder, not a complex freeform surface. From this design process, an optical system for an HUD having good performance is finally obtained. The size of the virtual image is 10 inches at 2 meters away from a combiner, and the area of the eye box is  $130 \times 50 \text{ mm}^2$ .

*Keywords* : Off-axis mirror system, Head-up display, Linear astigmatism

*OCIS codes* : (080.4035) Mirror system design; (080.0080) Geometric optics; (220.0220) Optical design and fabrication

## I. INTRODUCTION

Recently, many automobiles have been equipped with a head-up display (HUD) for reducing the distraction of the driver's attention and thus, car accidents [1]. The HUD system generally provides the information such as velocity, safety sign, and navigation in a form of virtual image for driving. Because the virtual image is located within the line of sight of the driver, it is always visible and helpful for the driver to get the information.

Since 1988, automobile makers have produced cars equipped with an HUD. Initially developed HUD systems had the limitations of color and contents, however, recently the HUD systems offer not only the information for driving but also the special function for interconnecting a smartphone [2].

The optical system for an HUD is generally designed to be an off-axis mirror system. This off-axis mirror system additionally generates the off-axial aberrations such as linear astigmatism. The off-axial aberrations can be corrected by using the freeform surface as an imaging mirror, however,

it is hard and expensive to manufacture the freeform mirror [3]. In this study, therefore, we propose a new optical element for an HUD system instead of the freeform mirror, through the initial design process based on the off-axial aberration analysis.

Using Chang's study, in the initial design stage we obtain an off-axis two-mirror system corrected for linear astigmatism [4, 5]. And then by introducing a conic surface into the secondary mirror, we additionally correct spherical aberration. Since the starting optical system for an HUD is corrected for dominant aberrations, namely, spherical aberration and linear astigmatism, it is easy to balance residual asymmetrical aberrations with a simple optical surface such as a cylinder, rather than a complex freeform surface. This design approach leads to an optical system having good performance to fulfill the requirements of an HUD system.

## II. CONSTRUCTION OF AN HUD SYSTEM

HUD systems are classified into two types. One is windshield-

\*Corresponding author: [separk@dankook.ac.kr](mailto:separk@dankook.ac.kr)



This is an Open Access article distributed under the terms of the Creative Commons Attribution Non-Commercial License (<http://creativecommons.org/licenses/by-nc/3.0/>) which permits unrestricted non-commercial use, distribution, and reproduction in any medium, provided the original work is properly cited.

type of which the image is projected on the windshield of an automobile. The other is combiner-type; its image is projected on an optical combiner. Both types are generally composed of an off-axis system including a display, mirror, and lens, as shown in Fig. 1.

Since the windshield is different for each model of automobiles, its HUD system should be developed to be matched to each automobile. Unfortunately, that increases the development cost. However, a combiner type is not dependent on what windshield is used, because of using a specific mirror, not a windshield. Therefore it can be widely available to various models of automobile. To apply to various models of automobile, in this study we propose a combiner-type HUD system designed using an off-axis two-mirror system.

To locate the virtual image at a feasible distance away from the driver, in addition to a combiner, at least one imaging mirror is required to enlarge the image source and to compensate the image error of the combiner. To recognize the information easily, a large virtual image is needed. The large virtual image can be acquired by enlarging the small image source of normally 0.6~1.8 inches LCD display and then projecting it onto the combiner. Here, we will design an HUD system having the virtual image of 10 inches at 2 meters away from the combiner, which is enlarged from a 1 inch LCD display.

When transitioning between the displayed driving information (virtual image) and the outside view, the driver can reduce the need to re-accommodate focus if the displayed distance is between 2 meters and 3 meters from the driver's eyes [6, 7]. Accordingly, in this study we locate the virtual image at 2 meters away from the combiner. Also, because

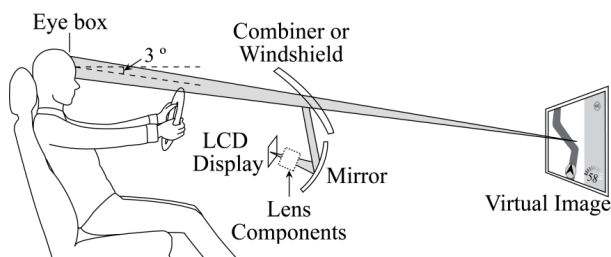


FIG. 1. Schematic diagram of an HUD optical system.

TABLE 1. Optical specification of an HUD optical system

Description	Unit	Current spec.	Designed spec.
Downward angle	deg.	3	3
Virtual image distance from combiner		2~2.5 m ahead	2 m ahead
Virtual image size	inch	3 ~ 8	10
Display size	inch	0.6~1.8	1
Eye box	mm <sup>2</sup>	130×50	130×50
Distortion	%	Under 3	1.4

the line of sight of the driver is tilted to the bottom, the virtual image is set to be projected with the downward angle of 3 degrees.

The area where a driver can easily recognize a virtual image is known as the eye box. Considering driver's eyes, we set the eye box of 130×50 mm<sup>2</sup>. The main specifications of an HUD system are summarized in Table 1.

### III. ABERRATIONS ANALYSES AND INITIAL DESIGN OF AN OFF-AXIS TWO-MIRROR SYSTEM

The optical system for an HUD is designed to be an off-axis system, of which the local coordinates are discontinuous at optical elements such as mirror and lens. In an off-axis single-mirror system, the tangential and sagittal image surfaces do not coincide, and they are tilted from the focal plane of the optical axis ray (OAR). The OAR is defined as the ray going from one focus to other focus, while passing through the aperture-stop center point and reflecting on the mirror. This astigmatic image's separation between the tangential and sagittal image surfaces is known as the linear astigmatism, from Chang's study [4, 5]. Since the linear astigmatism is the lowest-order aberration present in an off-axis single-mirror system and generates dominant image degradation, hence, it should primarily be corrected in the initial design stage.

As a specific example, consider an off-axis section of a paraboloidal mirror. The rays from an infinite object, after being reflected on the paraboloidal mirror, form the two tilted image surfaces, as shown in Fig. 2. Figure 3 shows its spot diagram. From these figures, we see that the linear astigmatism is the dominant aberration in an off-axis single-mirror system.

In an off-axis single-mirror system of Fig. 2, the tangential

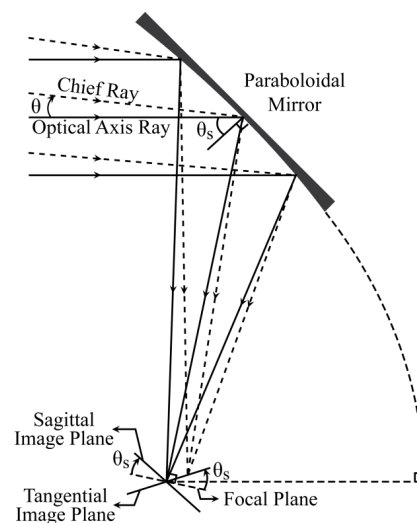


FIG. 2. Astigmatic image planes formed by an off-axis single-mirror.

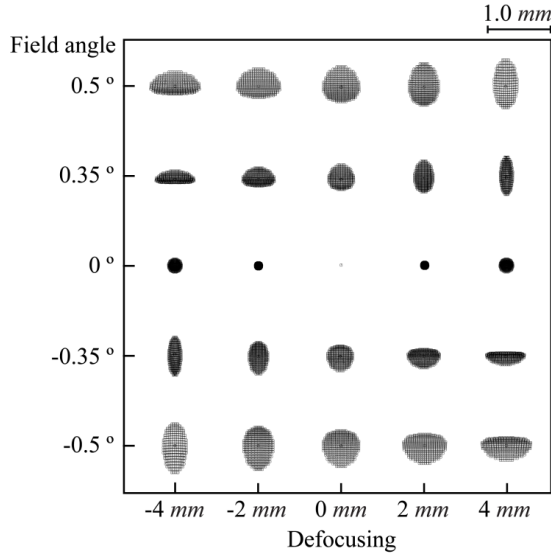


FIG. 3. Spot diagram of an off-axis single-mirror system.

( $s'_t$ ) and sagittal image distances ( $s'_s$ ) are respectively given by [4, 5]

$$\text{Tangential : } \frac{1}{s'_t} = \frac{2 \cos^2 \theta_s}{R} - \frac{1}{s} + \theta \frac{\sin 2\theta_s}{R} + \theta^2 \frac{1 + \sin^2 \theta_s}{R} + O(\theta^3), \quad (1)$$

$$\text{Sagittal : } \frac{1}{s'_s} = \frac{2 \cos^2 \theta_s}{R} - \frac{1}{s} - \theta \frac{\sin 2\theta_s}{R} - \theta^2 \frac{\cos^2 \theta_s}{R} + O(\theta^3), \quad (2)$$

where  $s$  is the object distance,  $\theta_s$  and  $\theta$  are the incidence angle of the optical axis ray and the field angle of the object in single-mirror system, respectively. Also,  $R$  is the radius of curvature of a paraboloidal mirror.

The linear astigmatism, expressed as astigmatic image's separation between  $s'_t$  and  $s'_s$  in Eqs. (1) and (2), can be corrected by an off-axis two-mirror system [4, 5]. Figure 4 shows the parameters of an off-axis two-mirror system. In this figure,  $i_1$  and  $i_2$  are the incidence angles of the optical axis ray at the primary mirror ( $M_1$ ) and the secondary mirror ( $M_2$ ), respectively. Also,  $\omega$  is the field angle of the object in an off-axis two-mirror system. In addition to them,  $l_1$  is the distance from  $M_1$  to the focus of  $M_1$ ,  $l_2$  is the distance from  $M_2$  to the focus of  $M_1$ . Here, if the focus of  $M_1$  is located in front of  $M_1$  (real image), then  $l_1$  is positive. Also, if the focus of  $M_1$  is behind  $M_2$  (virtual object), then  $l_2$  is negative.

In an off-axis two-mirror system of Fig. 4, the tangential ( $s'_{t2}$ ) and sagittal ( $s'_{s2}$ ) image distances from the secondary mirror are expressed as

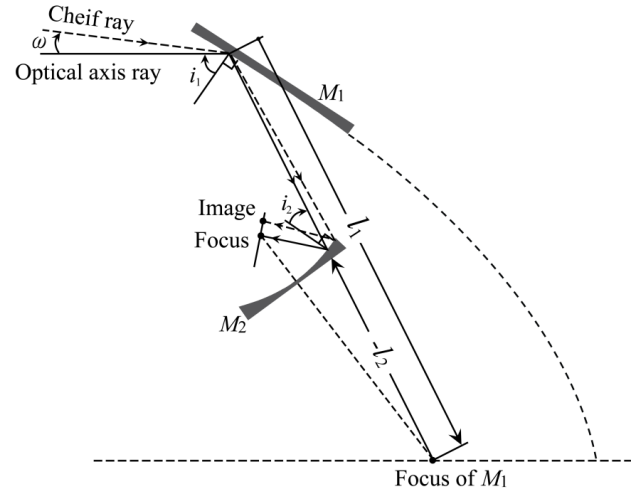


FIG. 4. Geometrical parameters of an off-axis two-mirror system.

$$\frac{1}{s'_{t2}} = -\frac{1}{s_{t2}} + \frac{2 \cos^2 i_2}{R_2} - \frac{\sin 2i_2}{R_2} \omega \left\{ -1 + \frac{l_1 + l_2}{l_2} + (l_1 + l_2) \left( \frac{1}{l_2} - \frac{1}{l_0} \right) \right\} + O(\omega^2), \quad (3)$$

$$\frac{1}{s'_{s2}} = -\frac{1}{s_{s2}} + \frac{2 \cos^2 i_2}{R_2} - \frac{\sin 2i_2}{R_2} \omega \left\{ 1 - \frac{l_1 + l_2}{l_2} + (l_1 + l_2) \left( \frac{1}{l_2} - \frac{1}{l_0} \right) \right\} + O(\omega^2), \quad (4)$$

where  $l_0$  is the distance between the secondary mirror and the system focus, measured along the OAR. Also,  $s_{t2}$  and  $s_{s2}$  are the tangential and sagittal object distances of the secondary mirror, and they are respectively given by [4, 5]

$$\frac{1}{s_{t2}} = \frac{1}{l_2} - \omega \left[ \frac{l_1}{l_2^2} (\tan i_1 + \tan i_2) + \frac{1}{l_2} \tan i_2 \right] + O(\omega^2), \quad (5)$$

$$\frac{1}{s_{s2}} = \frac{1}{l_2} + \omega \left[ \frac{l_1}{l_2^2} (\tan i_1 - \tan i_2) - \frac{1}{l_2} \tan i_2 \right] + O(\omega^2). \quad (6)$$

Inserting Eqs. (5) and (6) into Eqs. (3) and (4) results in an expression for the astigmatic image's separation  $\Delta s'_2$  of the off-axis two-mirror system:

$$\frac{\Delta s'_2}{s'_{t2} s'_{s2}} = 2\omega \frac{l_1}{l_2^2} \left( \frac{l_1}{R_1} \sin 2i_1 - \frac{l_2}{R_2} \sin 2i_2 \right) + O(\omega^2). \quad (7)$$

Since forcing  $\Delta s'_2 = 0$  in Eq. (7) makes the two image surfaces be the same without tilt, the condition for zero linear astigmatism is expressed as

$$\frac{l_1}{R_1} \sin 2i_1 = \frac{l_2}{R_2} \sin 2i_2. \tag{8}$$

In a single paraboloidal mirror system with an infinite object, spherical aberration does not exist at its focal point. In order to eliminate linear astigmatism, however, if the secondary mirror ( $M_2$ ) is added to form an off-axis two-mirror system, the spherical secondary mirror generates spherical aberration. Here, introducing the conic surface into  $M_2$  is very effective to correct spherical aberration. In Fig. 5, the focal point ( $O_2$ ) formed by the paraboloidal primary mirror corresponds to the object point of the secondary mirror, and then that is imaged onto  $O'_2$ . These object and image points are located on the same optical axis, therefore this system is rotationally symmetric with respect to the axis of the secondary mirror ( $M_2$ ).

Accordingly, for the third-order spherical aberration occurring at the secondary mirror, we can simply handle that with the rotational symmetry. The third-order spherical aberration coefficient ( $S_{I_2}$ ) induced by the spherical secondary mirror is expressed as [8-10]

$$S_{I_2} = (ni)^2_j y_j \left( \frac{u_j}{n_j} - \frac{u_{j-1}}{n_{j-1}} \right) \Big|_{j=2}. \tag{9}$$

In these equations,  $u_j$  and  $y_j$  are the convergence angle and height of the ray from the axial object point, and  $i$  is the angle between the axial ray and the surface normal at  $M_j$ , also  $n_j$  is the refractive index of the  $j$ th surface.

To correct spherical aberration of Eq. (9), the conic surface is introduced into the secondary mirror, with the equation given as

$$Z = \frac{ch^2}{1 + \sqrt{1 - (1+k)c^2 h^2}}, \tag{10}$$

where  $c$  is the curvature around the axis,  $h$  is the ray height on the conic surface, and  $k$  is a conic constant. Introducing the conic constant ( $k_j$ ) into the secondary mirror generates the additional third-order spherical aberration ( $\Delta S_{I_2}$ ), as follows [9, 10]:

$$\Delta S_{I_2} = (k_j c_j^3 h_j^4) (n_{j-1} - n_j) \Big|_{j=2}. \tag{11}$$

Therefore, the condition that the third-order spherical aberration is corrected, by combining Eq. (9) with Eq. (11), is expressed as follows [9, 10]:

$$k_2 = - \frac{S_{I_2}}{c_2^3 h_2^4 (n_1 - n_2)}. \tag{12}$$

In an initial design stage, the off-axis two-mirror system corrected for linear astigmatism and spherical aberration can be obtained by solving the parameters of Eqs. (8) and (12).

Figure 6 shows an off-axis two-mirror system corrected for linear astigmatism and spherical aberration, which is initially designed through the above design process. Also, the spot diagram of this system is illustrated in Fig. 7.

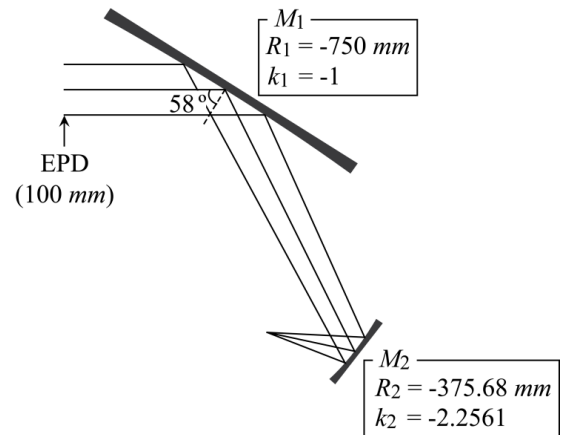


FIG. 6. Layout of an off-axis two-mirror system corrected for linear astigmatism and spherical aberration.

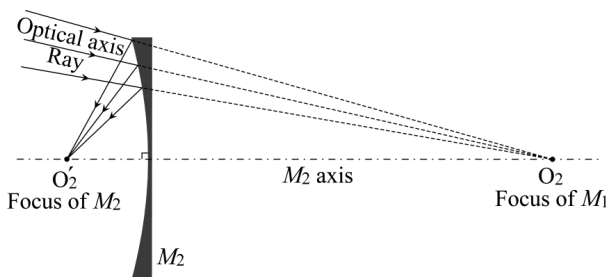


FIG. 5. Relationship between  $M_1$  and  $M_2$  foci.

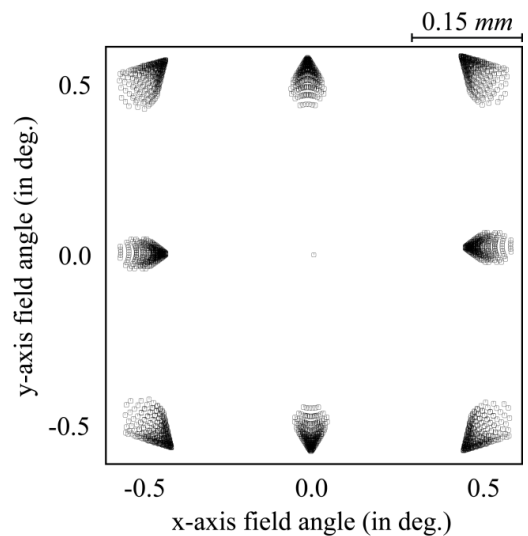


FIG. 7. Spot diagram of an off-axis two-mirror system corrected for linear astigmatism and spherical aberration.

Because the linear astigmatism and spherical aberration are corrected, this spot diagram shows that coma is the dominant aberration among the residual aberrations.

#### IV. COMPLETE DESIGN OF AN HUD OPTICAL SYSTEM

In designing an off-axis two-mirror system for an HUD, the locations of virtual image and LCD display are set to be the object and image surfaces, respectively. This configuration is to simplify the ray path in designing an off-axis mirror system. However, because all rays actually emanate from the LCD display, they are reversed conjugates.

The virtual image of an HUD is set to be placed at 2 meters away from the primary mirror (combiner) and interfered with the outside view. This configuration for the virtual image dramatically reduces the magnitude of accommodation due to the change of object distance.

In this study, the initial two-mirror system corrected for linear astigmatism and spherical aberration, mentioned in Section 3, is used as a starting system to design a final optical system for an HUD. Namely, the off-axis two-mirror system of Fig. 6 is optimized to meet the current specifications given in Table 1.

Because an HUD system is an off-axis system, its aberration properties are not rotationally symmetric. To balance this non-symmetrical aberration, most imaging mirrors have been designed by using the freeform surfaces [11]. Since the freeform surface has different aspheric coefficients in x-axis and y-axis, complex process and high cost are required to produce it [6, 12].

In this study, however, the freeform surface is not used. By aspherizing the secondary mirror, the aberrations of y-axis field have firstly been corrected. And after adding a cylindrical lens in front of the LCD display, we balance the aberrations of all fields including the x-axis field. Figure 8 and Fig. 9 show the layout and spot diagram of an HUD system, in which only the aberrations of the y-axis field are corrected, as shown in Fig. 9. This non-symmetrical aberrations results from the properties of the off-axis system for an HUD.

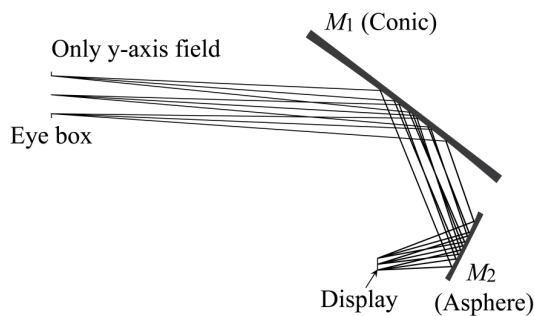


FIG. 8. Layout of an HUD system corrected for the aberrations of y-axis field only.

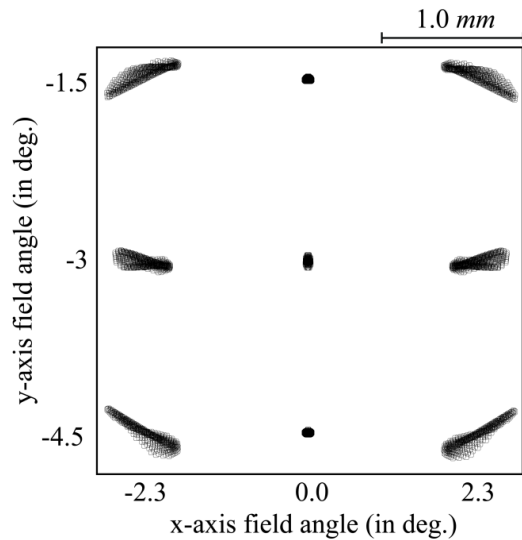


FIG. 9. Spot diagram of an HUD system corrected for the aberrations of y-axis field only.

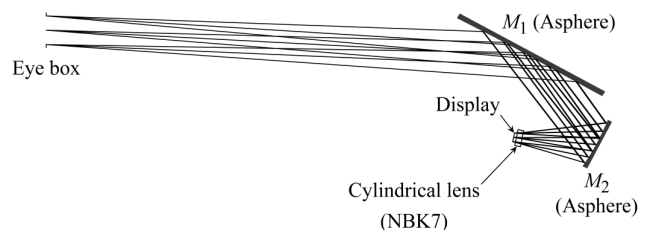


FIG. 10. Layout of a finally designed HUD system.

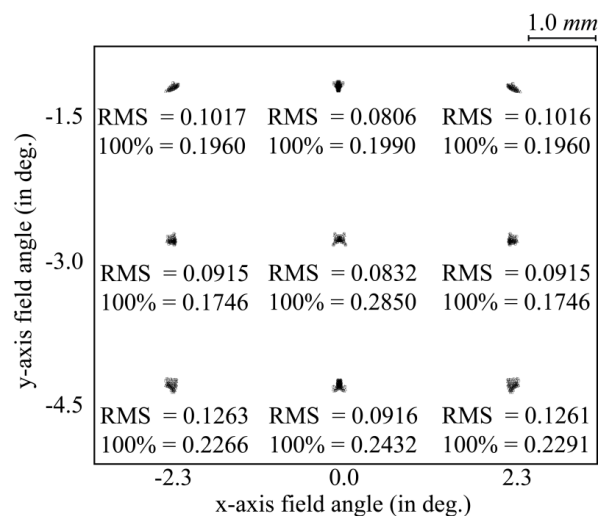


FIG. 11. Spot diagram of a finally designed HUD system (in mm).

To correct the aberrations of the x-axis field, a cylindrical lens having the x-axis curvature, not y-axis, is required and then added to an off-axis two-mirror system. Thus, we place the cylindrical lens near to the LCD display so that

TABLE 2. Surface design data of a finally designed HUD system (in mm).

Surface #	Y-Radius	X-Radius	Thickness	Description
Object	Infinite	Infinite	-2700.000	
Stop	Infinite	Infinite	700.000	
2	Infinite	Infinite	1128.675	
3	-659.850	-659.850	-329.925	Aspheric mirror
4	Infinite	Infinite	-1031.484	
5	-382.919	-382.919	-23.481	Aspheric mirror
6	Infinite	Infinite	-90.000	
7	Infinite	-61.267	-10.000	Cylindrical lens_NBK7
8	Infinite	Infinite	-5.000	
Image	Infinite	Infinite	0.000	

TABLE 3. Decenter data of a finally designed HUD system (in mm).

Surface #	Type	Y-decenter	$\alpha$ -tilt(degree)
3	Basic decenter	-1132.618	
4	Basic decenter		-52.978
6	Basic decenter	70.958	41.685
Image	Decenter and return	40.281	

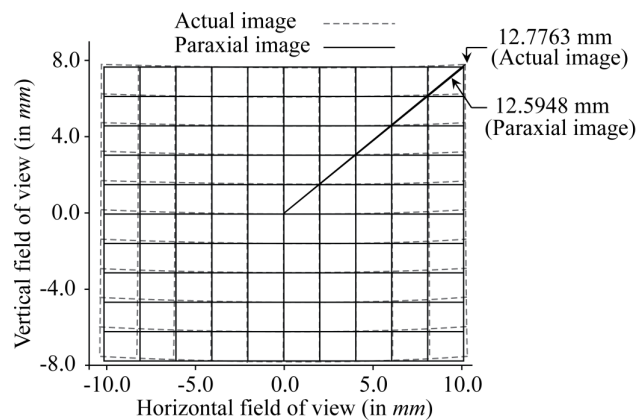


FIG. 12. Grid distortion of a finally designed HUD system on LCD display.

its size is reduced to  $26.2 \times 26.2 \text{ mm}^2$ . From this design process, an optical system for an HUD having good performance is finally obtained, and its layout is shown in Fig. 10. Compared to Fig. 9, aberrations at all fields are sufficiently balanced so that the RMS spot sizes at most fields are reduced to less than  $100 \mu\text{m}$ , as shown in Fig. 11.

Table 2 and Table 3 list the surface design data and the decenter data of a finally designed HUD system. In Table 3, “basic decenter” means that a new axis is defined for

current and succeeding surfaces after being decentered, and “decenter and return” denotes that only the current surface is decentered.

Figure 12 denotes the grid distortion of the finally designed system, in which distortion is less than 1.4% over all fields. Even though this system works in an off-axis system, distortion is so small that the distorted image is nearly not seen. Consequently, this system has good performance to fulfill the requirements of a head-up display system [13].

## V. CONCLUSION

By use of the aberration analysis for an off-axis mirror system implemented by Chang, this study suggests an off-axis optical system for a combiner-type HUD. In order to have a good initial design, the linear astigmatism, being dominant aberration in an off-axis single-mirror system, has firstly been corrected by adding another mirror to it. Furthermore, by introducing the conic surface into the secondary mirror, we eliminate the spherical aberration created by adding a spherical mirror.

To balance non-symmetrical aberration due to an off-axis mirror system, we added the cylindrical lens having the x-axis curvature to an off-axis two-mirror system, instead of a freeform surface. Also by placing this cylindrical lens near to the LCD display, its size is reduced to  $26.2 \times 26.2 \text{ mm}^2$ . From this design process, an optical system for an HUD having good performance is finally obtained. The size of virtual image is 10 inches at 2 meters away from a combiner, and the area of the eye box is  $130 \times 50 \text{ mm}^2$ .

As a result, this design method for an off-axis mirror system is expected to serve as a useful way to find design solutions for combiner- or windshield-type HUD if the specifications of the windshield are given to us.

## REFERENCES

1. H. Peng, D. Cheng, J. Han, C. Xu, W. Song, L. Ha, J. Yang, Q. Hu, and Y. Wang, “Design and fabrication of a holographic head-up display with asymmetric field of view,” *Appl. Opt.* **53**, H177-H185 (2014).
2. V. Milanovic, A. Kasturi, and V. Hachtel, “High brightness MEMS mirror based head-up display (HUD) modules with wireless data streaming capability,” *Proc. SPIE* **9375**, 93750A (2015).
3. T. Y. Kim, M. H. Shin, and Y. J. Kim, “Design of off-axis wide angle lens for the automobile application,” *J. Opt. Soc. Korea* **17**, 336-343 (2013).
4. S. Chang and A. Prata, Jr., “Geometrical theory of aberrations near the axis in classical off-axis reflecting telescopes,” *J. Opt. Soc. Am.* **22**, 2454-2464 (2005).
5. S. Chang, “Geometrical theory of aberrations for classical offset reflector antennas and telescopes,” Dissertation of Ph. D. Degree, University of Southern California (2003).
6. P. Ott, “Optic design of head-up displays with freeform

- surfaces specified by NURBS,” Proc. SPIE **7100**, 71000Y (2008).
7. L. Lacoste, D. Stindt, and E. Buckley, “Head up displays,” U. S. Patent 20120224062A1 (2012).
  8. W. J. Smith, *Modern Optical Engineering*, 3rd ed. (McGraw-Hill Inc., New York, USA, 2001), Chapter 2, 3, 10.
  9. W. T. Welford, *Aberrations of the Optics Systems* (Adam Hilger Ltd., Bristol, UK, 1986), pp. 130-158.
  10. K. H. Kim, Y. S. Kim, and S. C. Park, “Design of a tele-centric wide field lens with high relative illumination and low distortion using third-order aberration analysis,” J. Opt. Soc. Korea **19**, 679-686 (2015).
  11. H. Hoshi, N. Taniguchi, H. Morishima, and T. Akiyama, “Off-axial HMD optical system consisting of aspherical surfaces without rotational symmetry,” Proc. SPIE **2653**, 234-242 (1996).
  12. F. Z. Fang, X. D. Zhang, and X. T. Hu, “Cylindrical coordinate machining of optical freeform surfaces,” Opt. Express **16**, 7323-7329 (2008).
  13. J. M. Ryu, “Optical system for head up display,” Korea Patent 1020130127799 (2013).